



## Unipolar Charging of Aerosol Particles in the Size Range of 75-500 nm by Needle-plate Corona Charger

ALEXEY ANATOLEVICH EFIMOV<sup>1\*</sup>, PAVEL VLADIMIROVICH ARSENOV<sup>1</sup>,  
TOMAS MAEDER<sup>1,2</sup> and VICTOR VLADIMIROVICH IVANOV<sup>1</sup>

<sup>1</sup>Department of Physical and Quantum Electronics, Moscow Institute of Physics and Technology, Dolgoprudny 141701, Russia.

<sup>2</sup>Ecole Polytechnique Federale de Lausanne, Lausanne CH-1015, Switzerland.

\*Corresponding author E-mail: efimov.aa@mipt.ru.

<http://dx.doi.org/10.13005/ojc/340124>

(Received: November 26, 2017; Accepted: December 29, 2017)

### ABSTRACT

A simple unipolar needle-plate corona charger (NPC) was designed, fabricated and tested on aerosol  $Al_2O_3$  particles in the size range 75-500 nm. The intrinsic charging efficiency, particle electrostatic losses, and extrinsic charging efficiency were investigated depending on the corona current (35-215  $\mu$ A), corona polarity, and aerosol flow rate (12-250 l/min). It was found that the intrinsic charging efficiency of the NPC is growing with increase in the corona current and the particle size and decrease in the aerosol flow rate. However, the extrinsic charging efficiency is lower than intrinsic one due to the particle electrostatic losses. Although the NPC has very simple design, it provides the extrinsic charging efficiency comparable with that of unipolar corona chargers of other types having more complicated design. The maximum value of the extrinsic charging efficiency was more than 40% for particles in the size range from 98 to 210 nm.

**Keywords:** Unipolar Charging, Needle-plate Corona Charger, Aerosol Particles, Charging efficiency.

### INTRODUCTION

Particle charging is one of the most important processes in aerosol science and technology. Nowadays particle charging is successfully used for the particle size measurements<sup>1</sup>, formation of functional structures<sup>2</sup>, synthesis of nanoparticles<sup>3</sup>, electrostatic air filtration<sup>4,5</sup>, and many other processes. It is known

that high particle charging efficiency is achieved by using unipolar corona chargers. A recent extensive review of unipolar corona chargers is available in the article by Intra *et al.*,<sup>6</sup> There are two main types of unipolar corona chargers. In the first type of unipolar corona chargers, the generation and collision of ions with particles is performed in various zones of the charger. In this regard, these chargers have low values for particle losses.



However, these chargers have also a low charging efficiency due to ion losses during their transport to the particle zone. In the second type of chargers called direct unipolar corona chargers<sup>7</sup>, the generation and collision of ions with particles takes place in one discharge zone. As a result, because of reduced ion losses high-efficiency charging of aerosol particles is achieved. Moreover, the manufacturing of these types of unipolar corona chargers is much cheaper due to a simple design. For this reason, in this study we developed and investigated unipolar corona charger of the second type as the most promising device for charging particles.

Compared to other chargers<sup>8-11</sup>, developed and evaluated corona unipolar charger has a simple design. As a result, this charger has a lower cost of fabrication and maintenance. The concept of simple design, mentioned in this paper means that the design of the charger consists of a minimum number of working parts, which are the standard products (needle, tube, plate, etc.). In contrast, the complicated design of the charger needs to use special parts requiring high precision of manufacturing (milling, drilling, turning treatment, etc.). Intrinsic charging efficiency, particle electrostatic losses and extrinsic charging efficiency of particles in the size range from 75 to 500 nm were investigated depending on the corona current from 35 to 215  $\mu\text{A}$ , corona polarity (negative/positive) and aerosol flow rate through the charger from 12 to 250 l/minutes.

## EXPERIMENTAL

The scheme of the experiment on the study of a unipolar corona charger using a needle-plate (NPC) is shown in Fig. 1. The experiment was carried out as follows: the aerosol particles (i.e.  $\text{Al}_2\text{O}_3$ ) with the size from 75 to 500 nm were generated by using a multi-spark discharge generator (m-SDG), and then sent to the NPC. Next, the charged aerosol was passed through the electrostatic precipitator (ESP) and at the exit of which the number concentration of particles was measured with an aerosol spectrometer (AS). The particle concentration was measured more than 5 times to reduce measurement uncertainty. The intrinsic charging efficiency  $\zeta_{\text{intr}}$ , particle electrostatic

losses  $L_E$  and extrinsic charging efficiency  $\zeta_{\text{extr}}$  can be expressed as follows<sup>8</sup>

$$\eta_{\text{intr}} = \frac{n_1 - n_2}{n_1}, \quad (1)$$

$$L_E = \frac{n_1 - n_2}{n_1}, \quad (2)$$

$$\eta_{\text{extr}} = \eta_{\text{intr}} - L_E, \quad (3)$$

where  $n_1$  – the particle number concentration measured when the NPC and the ESP were turned off;

$n_2$  – the particle number concentration measured when the NPC was turned on, but the ESP was turned off;

$n_3$  – the particle number concentration measured when the NPC and the ESP were turned on.

Since these parameters (i.e.  $\zeta_{\text{intr}}$ ,  $L_E$  and  $\zeta_{\text{extr}}$ ) are often used in practice, they are chosen as main characteristics for evaluating the performance of the NPC. For example, intrinsic charging efficiency  $\zeta_{\text{intr}}$  is the number fraction of originally neutral particles which acquire a charge within the charger regardless of whether the particles leave the charger or not. Particle electrostatic losses  $L_E$  is the number fraction of charged particles that are lost in the charger due to electrical forces. Extrinsic charging efficiency  $\zeta_{\text{extr}}$  is the number fraction of originally neutral particles which appear at the outlet of the charger carrying at least a unit of charge. Therefore, the last parameter is the most important for practical applications.

A developed charger consisted of a needle and a plate that were located in a dielectric polyvinyl chloride tube with an internal diameter of 45 mm. In comparison with other chargers<sup>9-11</sup>, this simple design means more reliable operation, since it contains a smaller number of moving and/or wearing parts. A steel needle with a radius of curvature of about 40  $\mu\text{m}$  was used as the corona electrode. The needle was located at a distance of 10 mm from the steel plate with a size of 100 x 30 x 2 mm. The distance between the needle and plate was chosen experimentally for achieving of the maximum current of a corona discharge from 35 to

215  $\mu\text{A}$ . A region of high electric field strength was created between the needle and the plate when a high voltage of 5 to 16 kV was applied to the needle. As a result, there is an ionization of the gas molecules and ignition of a corona discharge. Positive and negative corona discharge was created when the positive and negative potentials

were applied to the needle, respectively. Aerosol nanoparticles adsorbed unipolar charge due to collisions with ions or electrons, depending on the polarity of the corona electrode<sup>12</sup>. The source of high voltage was the source of VIDN-30 (up to 30 kV and 250  $\mu\text{A}$ ), and the corona discharge current was measured with an Agilent U1253B multimeter.

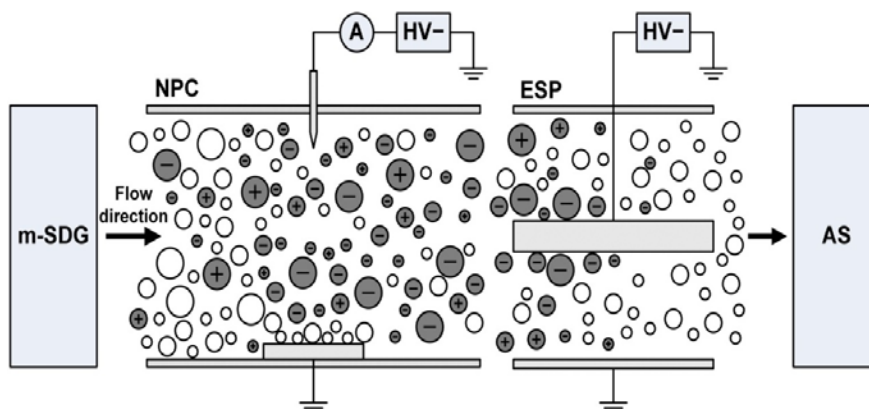


Fig. 1. The scheme of the experiment on the study of a unipolar corona charger using a needle-plate (m-SDG – multi-spark discharge generator, NPC – needle-plate corona charger, ESP – electrostatic precipitator and AS – aerosol spectrometer).

The current-voltage characteristic of the charger is shown in Fig. 2. The electric breakdown of the gap occurred at a voltage between the needle and the plate equal to 16 and 9 kV at negative and positive polarity, respectively (Fig. 2). The lower value of the breakdown voltage with the use of positive polarity is explained by the formation of a positive space charge at the point, which is described in detail by other authors<sup>13,14</sup>. An electrostatic precipitator is a cylindrical capacitor having a length, inner and outer diameter equal to 1000, 10 and 50 mm, respectively. In the electrostatic precipitator the deposition of all charged particles was carried out to determine the fraction of charged particles in the aerosol (see Eq. 1-3). The voltage between the electrodes of the electrostatic precipitator was 10 kV. Commercial aerosol spectrometer TSI SMPS 3936 was used to determine the size and concentration of aerosol particles. The parameters of the charger were investigated by varying the corona discharge current  $I_c$  from 35 to 215  $\mu\text{A}$ , charging polarity (negative and positive), and aerosol flow rate  $Q_a$  through the charger from 12 to 250 l/min. for a particle size range of 75 to 500 nm. The particle size range from 75 to 500 nm is typical for

agglomerates obtained with a multi-spark discharge generator<sup>15,16</sup>. Aerosol particles were obtained by the erosion of the electrodes made of Al in air at energy stored in the capacitor and the repetition rate of discharges equal to 6 J and 1 Hz, respectively.

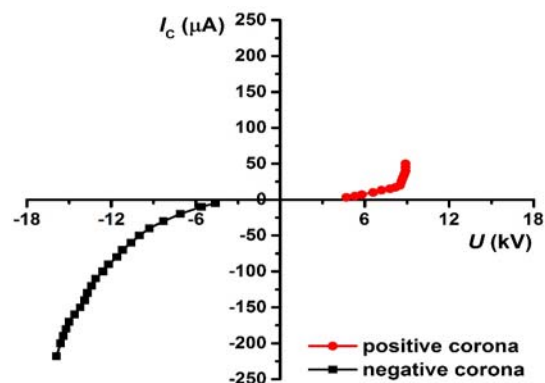


Fig. 2. Voltage-current characteristics of the NPC at needle-plate spacing is about 10 mm

## RESULT AND DISCUSSION

### The influence of the discharge current

Figure. 3 shows a graph of the effect of corona discharge current  $I_c$  on intrinsic charging

efficiency  $\zeta_{\text{intr}}$ , particle electrostatic losses  $L_E$  and extrinsic charging efficiency  $\zeta_{\text{extr}}$  of particles with sizes from 75 to 500 nm in the charger with a negative polarity corona and the aerosol flow rate  $Q_a$  is 33 l/min. It should be noted that a similar dependence was obtained at positive polarity corona discharge and the aerosol flow rate  $Q_a$  is equal to 12 and 250 l/min. respectively.

Figure. 3a shows that when increasing the current  $I_c$  from 35 to 215  $\mu\text{A}$ , the intrinsic charging efficiency  $\zeta_{\text{intr}}$  also increases for all particle sizes in the range from 75 to 500 nm. For example, the intrinsic charging efficiency  $\zeta_{\text{intr}}$  of particles with size of 75 nm is increased from 57.8% to 96.1% with increasing discharge current  $I_c$  from 35 to 215  $\mu\text{A}$ , respectively. This result is explained by an increase in the probability of collisions of particles with ions/electrons due to an increase in their concentration with the discharge current<sup>17</sup>. Fig. 3a also shows that the most efficiently charged particles of the submicron range of sizes, namely with particle sizes of more than 225 nm, the intrinsic charging efficiency  $\zeta_{\text{intr}}$  of their charging increases with the size and reaches almost 100%. In accordance with the theory of charging<sup>18</sup>, increasing the charging efficiency of particles is caused by the increase in the probability of collision of the particles with ions/electrons, due to an increase in their size. For example, in an electric field with a strength of 5 kV/cm and an ion/electron concentration of  $10^7 \text{ cm}^{-3}$  during 1 s, a particle with a size of 40 and 400 nm adsorbs about 0.26 and 25.9 elementary charges, respectively, according to Hinds<sup>17</sup>. However, it is seen that a significant proportion of charged particles more than 75% larger than 225 nm is deposited in the charger as a result of electrostatic losses (Fig. 3b). Typically, these losses are due to the high electrical mobility of the particles because the high electrical mobility of the particles is the result of a large number of charges on the particles<sup>17</sup>. As a result, it can be concluded that due to high electrostatic losses  $L_E$ , the extrinsic charging efficiency  $\zeta_{\text{extr}}$  of particles larger than 225 nm becomes substantially lower than their intrinsic charging efficiency  $\zeta_{\text{intr}}$  (Fig. 3ab). Since the extrinsic charging efficiency  $\zeta_{\text{extr}}$  is determined by the difference between the intrinsic charging efficiency  $\zeta_{\text{intr}}$  and particle electrostatic

losses  $L_E$ , see Eq. 3. Experimental measurements showed that the extrinsic charging efficiency  $\zeta_{\text{extr}}$  reaches a maximum value at the low value of the discharge current  $I_c$  about 35 mA, and the value of the extrinsic charging efficiency  $\zeta_{\text{extr}}$  of particles increases with decreasing particle size (Fig. 3b). As a result, the developed charger is recommended to be used for charging particles smaller than 225 nm at low current values of about 35  $\mu\text{A}$ , and this result agrees with the conclusions from other experimental works<sup>8,9</sup>.

### The influence of the polarity of the corona discharge

Figure. 4 shows the effect of polarity of the corona discharge on intrinsic charging efficiency  $\zeta_{\text{intr}}$ , particle electrostatic losses  $L_E$  and extrinsic charging efficiency  $\zeta_{\text{extr}}$  of particles with sizes from 75 to 500 nm in the charger, when the corona current  $I_c$  and the aerosol flow rate  $Q_a$  are 35  $\mu\text{A}$  and 33 l/min, respectively. Similar dependences were obtained at a corona current  $I_c$  and aerosol flow rate  $Q_a$  equal to 100-215  $\mu\text{A}$  and 12-250 l/min, respectively.

Figure. 4a shows that the intrinsic charging efficiency  $\zeta_{\text{intr}}$  is a few percent higher for negative corona in comparison with positive corona for all particles in the size range from 75 to 500 nm. This result agrees with the data obtained by other researchers<sup>19,20</sup> and is probably associated with a higher electrical mobility of negative ions/electrons, leading to an increase in the charging efficiency. It should be noted that the particle electrostatic losses  $L_E$  by using a negative corona is also higher than in the case of positive corona (Fig. 4b). So, for example, electrostatic losses of particles of size 100 nm is 36.6% and 15.5% at the positive and negative corona, respectively. In addition, the results of the measurements testify that the extrinsic charging efficiency  $\zeta_{\text{extr}}$  has higher values for particles in the size range from 75 to 98 nm at a negative corona polarity. However, higher values of extrinsic charging efficiency  $\zeta_{\text{extr}}$  for particles in the size range from 98 to 500 nm are achieved at a positive corona polarity. For example, the extrinsic charging efficiency  $\zeta_{\text{extr}}$  more than 40% was achieved for particles in the size range from 98 to 210 nm, see Fig. 4c. Thus, it is possible to choose an effective charging mode by changing the polarity of the corona.

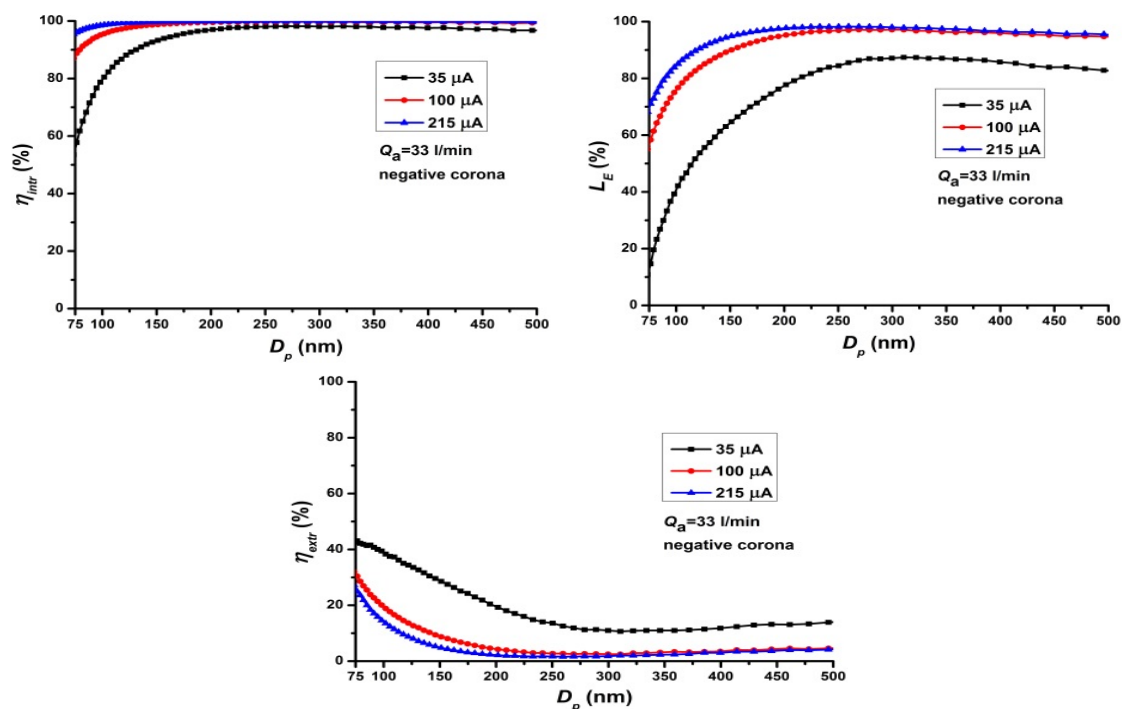


Fig. 3. Effect of corona current  $I_c$  on intrinsic charging efficiency  $\zeta_{intr}$  (a), particle electrostatic losses  $L_E$  (b) and extrinsic charging efficiency  $\zeta_{extr}$  (c) as a function of particle size from 75 to 500 nm. Negative corona,  $Q_a = 33$  l/minutes

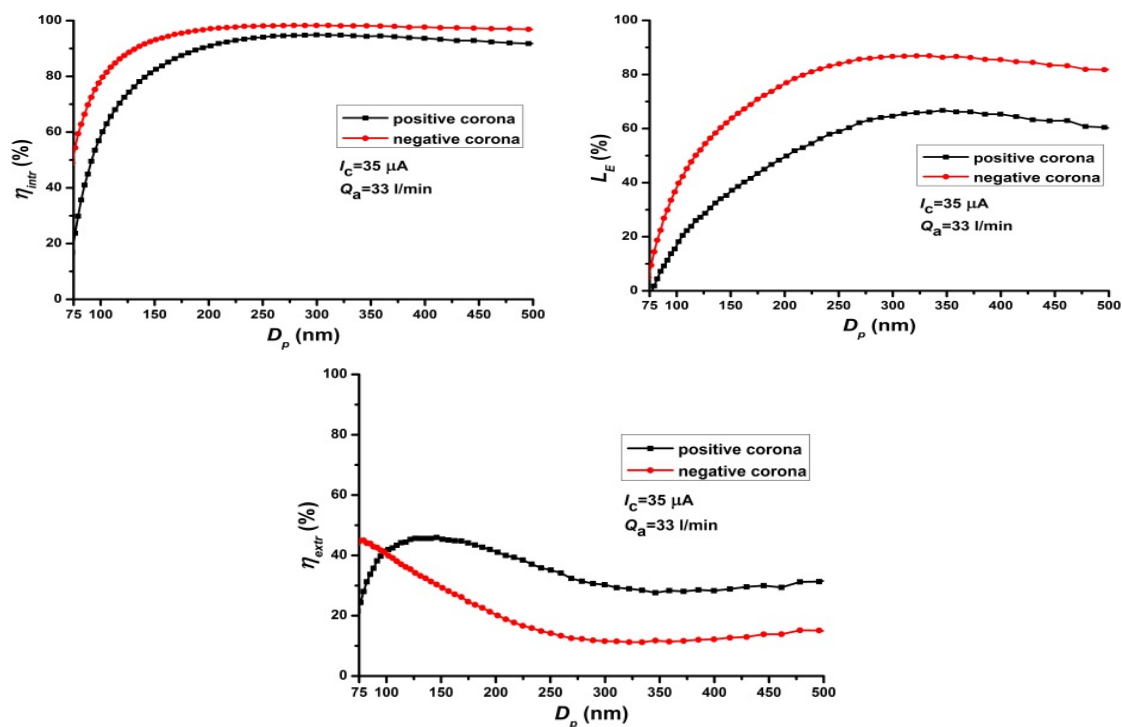


Fig. 4. Effect of corona polarity on intrinsic charging efficiency  $\zeta_{intr}$  (a), particle electrostatic losses  $L_E$  (b) and extrinsic charging efficiency  $\zeta_{extr}$  (c) as a function of particle size from 75 to 500 nm at  $I_c = 35$   $\mu$ A and  $Q_a = 33$  l/minutes

### The influence of the aerosol flow rate through the charger

Figure. 5 shows the effect of aerosol flow rate  $Q_a$  on intrinsic charging efficiency  $\zeta_{intr}$ , particle electrostatic losses  $L_E$  and extrinsic charging efficiency  $\zeta_{extr}$  of particles with sizes from 75 to 500 nm in the charger with a negative polarity corona and the corona current  $I_c=215 \mu\text{A}$ . Similar dependences were obtained at a positive corona and corona current  $I_c$  equal to 35-100  $\mu\text{A}$ .

Figure. 5a shows that extrinsic charging efficiency  $\zeta_{extr}$  decreases with increasing aerosol flow rate  $Q_a$  from 12 to 250 l/min. for particles in the size range from 75 to 500 nm. This happens as a result of decreasing of residence time of the particles in the charger and hence the probability of particle collisions with ions/electrons is reduced.

Similarly, particle electrostatic losses  $L_E$  also decreases while increasing aerosol flow rate  $Q_a$  because the particles will have less time to reach the grounded plate (Fig. 5b).

The effect of the aerosol flow rate  $Q_a$  on particle electrostatic losses  $L_E$  has more impact than on the intrinsic charging efficiency  $\zeta_{intr}$  (Fig. 5a and 5b, respectively). For example, the intrinsic charging efficiency  $\zeta_{intr}$  for 300 nm particles decreases from 99.9% to 97.4%, while the particle electrostatic losses  $L_E$  is reduced from 99.2% to 84.2% when increasing the aerosol flow rate  $Q_a$  from 12 to 250 l/min. respectively. As a result, the extrinsic charging efficiency  $\zeta_{extr}$  increases with increasing aerosol flow rate  $Q_a$ , mainly due to reduced losses (Fig. 5c). Thus, a more efficient mode of operation of the charger is achieved.

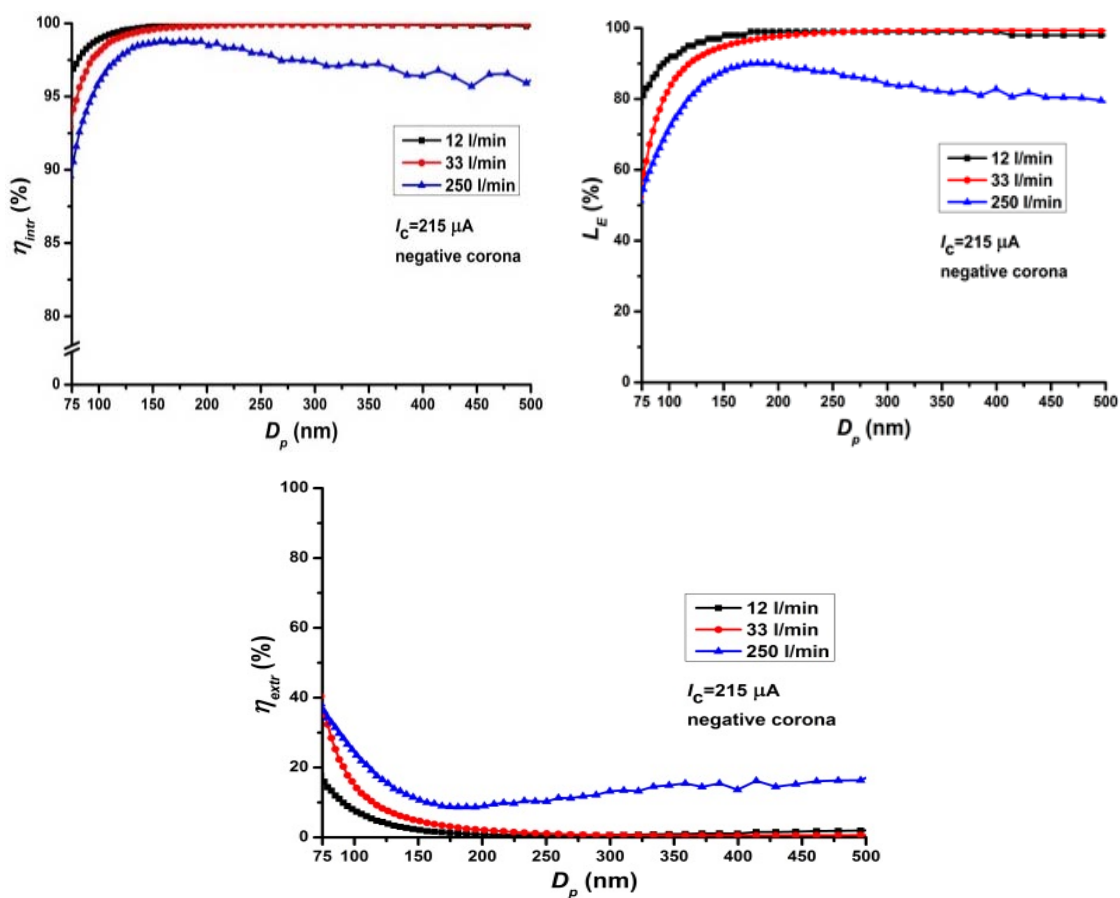


Fig. 5. Effect of aerosol flow rate  $Q_a$  on intrinsic charging efficiency  $\zeta_{intr}$  (a), particle electrostatic losses  $L_E$  (b) and extrinsic charging efficiency  $\zeta_{extr}$  (c) as a function of particle size from 75 to 500 nm. Negative corona,  $I_c=215 \mu\text{A}$ .

### Comparison of chargers

Comparison of the extrinsic charging efficiency  $\zeta_{\text{extr}}$  of present charger with other previous results<sup>8-11</sup> is shown in Fig. 6. The developed unipolar charger demonstrates a higher extrinsic charging efficiency  $\zeta_{\text{extr}}$  than a bipolar charger with positive and negative ions<sup>10</sup> (Fig. 6). This result confirms that the developed charger operates in unipolar charging mode. The developed unipolar charger demonstrates almost the same extrinsic charging efficiency  $\zeta_{\text{extr}}$  in comparison with other unipolar chargers<sup>8,9,11</sup> for particle size range from

75 to 500 nm (Fig. 6). It is known that the value of the extrinsic charging efficiency  $\zeta_{\text{extr}}$  depends on the operating parameters of the chargers. In this regard, the main parameters of the chargers, such as the current  $I_c$  or voltage, corona polarity and the aerosol flow rate  $Q_a$  are also indicated in Fig. 6. Thus, the developed unipolar charger with a simple design consisting of standard products (polyvinyl chloride tube, steel needle, plate, etc.) is a good alternative to other chargers that have a more complex design and high cost.

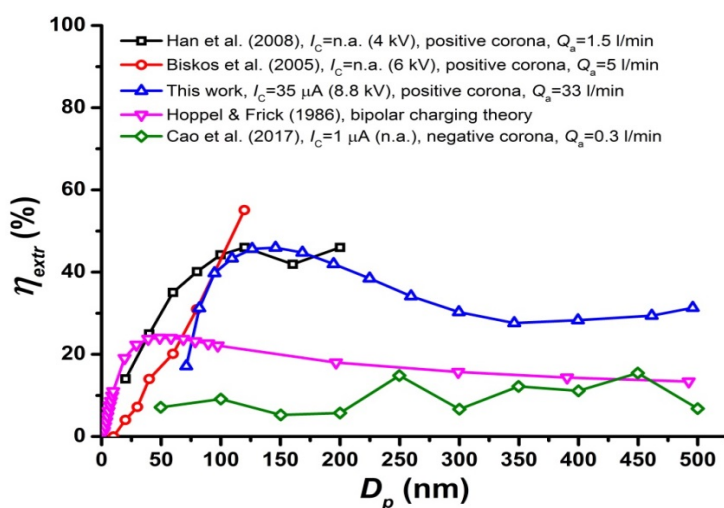


Fig. 6. Comparison of the extrinsic charging efficiency  $\zeta_{\text{extr}}$  of present charger at  $I_c=35 \mu\text{A}$  (8.8 kV), positive corona and  $Q_a=33 \text{ l/min}$  with other previous results as a function of particle size

### CONCLUSION

A simple unipolar charger of aerosol particle consisting of a needle and a plate in the tube was designed, fabricated and evaluated. Three parameters, including intrinsic charging efficiency, particle electrostatic losses, and extrinsic charging efficiency were evaluated depending on the operating mode of the charger. It was found that the intrinsic charging efficiency increases up to 100% with increasing corona current from 35 to 215  $\mu\text{A}$ , reducing the aerosol flow rate from 250 to 12 l/min. and increasing the particle size from 75 to 500 nm. It was also found that the intrinsic charging efficiency with the use of a negative corona is higher than in the case of a positive corona. It is established that extrinsic charging efficiency is lower than the

intrinsic charging efficiency due to high values of particle electrostatic losses. The maximum value of the extrinsic charging efficiency was about 40% for particle size range from 75 to 500 nm. The developed charger demonstrated almost the same extrinsic charging efficiency in comparison with other unipolar chargers. In addition, the developed unipolar charger has a simple design, which enables its use in a wide range of aerosol charging and neutralizing applications. It is important for a wide range of applications of charged particles.

### ACKNOWLEDGEMENT

This work was supported by the Russian Science Foundation (project No. 15-19-00190).

## REFERENCES

1. Wang, S. C.; Flagan, R. C. *Aerosol Sci. Technol.*, **1990**, *13*, 230–240.
2. Park, J.; Jeong, J.; Kim, C.; Hwang, J. *Aerosol Sci. Technol.*, **2013**, *47*, 512–519.
3. Park, K.-T.; Farid, M. M.; Hwang, J. *J. Aerosol Sci.*, **2014**, *67*, 144–156.
4. Efimov, A. A.; Ivanov, V. V.; Volkov, I. A.; Subbotina, I. R.; Pershin, N. A. *Nanotechnologies Russ.*, **2013**, *8*, 789–798.
5. Bologna, A.; Paur, H.-R.; Seifert, H.; Wäscher, T.; Woletz, K. *J. Electrostat.*, **2009**, *67*, 150–153.
6. Intra, P.; Tippayawong, N. *J. Electrostat.*, **2009**, *67*, 605–615.
7. Alonso, M.; Huang, C. H. *J. Nanoparticle Res.*, **2015**, *17*, 1–8.
8. Han, B.; Kim, H.-J.; Kim, Y.-J.; Sioutas, C. *Aerosol Sci. Technol.*, **2008**, *42*, 793–800.
9. Biskos, G.; Reavell, K.; Collings, N. *J. Aerosol Sci.*, **2005**, *36*, 247–265.
10. Hoppel, W. A.; Frick, G. M. *Aerosol Sci. Technol.*, **1986**, *5*, 1–21.
11. Cao, Y. Y.; Wang, H. Q.; Sun, Q.; Qin, F. H.; Gui, H. Q.; Liu, J. G.; Wang, J.; Lü, L.; Kong, D. Y.; Yu, T. Z. *IOP Conf. Ser. Earth Environ. Sci.*, **2017**, *69*, 12174.
12. Plasma Physics and Engineering, Second Edition. *CRC Pres.*, **2011**.
13. Sadaoui, F.; Beroual, A. In *2012 International Conference on High Voltage Engineering and Application.*, **2012**, 496–499.
14. Xiao, D. In *Gas Discharge and Gas Insulation; Energy and Environment Research in China*; Springer, Berlin, Heidelberg., **2016**, 149–194.
15. Efimov, A.; Lizunova, A.; Sukharev, V.; Ivanov, V. *Korean J. Mater. Res.*, **2016**, *26*, 123–129.
16. Efimov, A.; Sukharev, V.; Ivanov, V.; Lizunova, A. *Orient. J. Chem.*, **2015**, *31*(4), 2285-2290.
17. Hinds, W. C. *Aerosol Technology: Properties, Behavior, and Measurement of Airborne Particles*; 2 edition.; Wiley-Interscience: New York., **1999**.
18. Fuchs, N. A. *Geofis. Pura E Appl.*, **1963**, *56*, 185–193.
19. Adachi, M.; Kousaka, Y.; Okuyama, K. *J. Aerosol Sci.*, **1985**, *16*, 109–123.
20. Hernandez-Sierra, A.; Alguacil, F. J.; Alonso, M. *J. Aerosol Sci.*, **2003**, *34*, 733–745.